

Role of Population Noise on the Transient Statistics of a CO₂ Laser near Threshold.

M. CIOFINI, R. MEUCCI, PENG-YE WANG(*) and F. T. ARECCHI(**)

Istituto Nazionale di Ottica - Largo E. Fermi 6, 50125 Firenze, Italy

(received 29 June 1992; accepted in final form 29 December 1992)

PACS. 05.40 – Fluctuation phenomena, random processes, and Brownian motion.

PACS. 42.55D – CO₂ lasers.

PACS. 42.50 – Quantum optics.

Abstract. – We present experimental evidence of a two-peaked passage time distribution in a *Q*-switched single-mode CO₂ laser. This novel feature occurs when the initial setting of the net laser gain is close to the threshold value. Population fluctuations with a decay time longer than the transient duration explain this phenomenon.

Transient statistics is a powerful method to investigate fundamental processes in non-equilibrium systems. The method was first applied to study the transient evolution of the photon number statistics in a *Q*-switched He-Ne laser [1], showing an anomalous variance due to the deterministic amplification of the initial statistical spread.

Later, passage time statistics was introduced to study the influence of quantum noise in macroscopic systems [2]. In a laser the passage time is defined as the time between the instant at which the control parameter is changed ($t = 0$) and that at which the photon number reaches a pre-assigned value. By this method the statistical properties of radiation growth in several types of lasers were explored [3-6]. Further work includes theoretical considerations about additive and multiplicative noise [7] and measurements of the transient statistics of semiconductor lasers [8].

In a recent paper [9] we have shown a new feature, namely the appearance of a two-peaked passage time distribution in the transient onset of a single-mode CO₂ laser. Two-peaked distributions had also been observed in dye [10] and semiconductor [11] lasers, however, in the former case two-peaked passage time distributions arose from the coupling between two transverse modes, and in the latter case they were induced by the correlation between two successive modulation pulses. The general explanation for this new effect is that population fluctuations in class-*B* laser live longer than the transient duration, hence any initial-population peculiarity remains frozen for the whole transient, whereas in a class-*A* laser (as *e.g.* He-Ne, or dye) it would be rapidly washed out. In ref. [9] it was shown how,

(*) Permanent address: Institute of Physics, Academia Sinica, Beijing, China.

(**) Also at Department of Physics, University of Florence, Italy.

starting from a suitable initial condition close to threshold, the two-peak separation varies as a function of the final setting of the gain.

In this letter we show how the two-peak character depends on the initial setting close to threshold, and provide a theoretical model as well as a heuristic explanation for these phenomena.

The experimental set-up consists of a single-mode CO₂ laser excited by means of a DC discharge. The cavity losses are switched by an intracavity electro-optic modulator driven with a square wave of 100 Hz frequency and 40 ns rise time. At $t = 0$ the cavity loss parameter k is switched from a high value k_0 to a low value k_1 . The laser pulse is detected by a Hg-Cd-Te photodiode with a rise time less than 10 ns. The photon number n at which the passage time is measured is set to $n = n_s/2$, n_s being the saturation value [6].

For a selected discharge current, we adjust k_0 in order to start close to threshold. That means to set the initial net gain $a_0 = G\Delta_0/2 - k_0$ close to zero. Here $G = 4.6 \cdot 10^{-8}$ is the field-matter coupling constant and Δ_0 is the population inversion estimated via the relation $\Delta_0 = Mi$, i being the discharge current and $M = 2.00 \cdot 10^{14} \text{ mA}^{-1}$ [9].

Figure 1 shows how the passage time distributions are modified as we change the initial gain around threshold. We do it by setting the discharge current by an amount Δi from the threshold value i_{th} , and report three experimental cases for $\Delta i/i_{\text{th}} = -0.4\%$, -0.1% , and $+0.4\%$, respectively. In fig. 2 we report the stationary laser output at fixed losses for different discharge currents i , and extrapolate the threshold current $i_{\text{th}} \approx 4.30 \text{ mA}$ from points rather above threshold. We have checked that the two-peaked structure is not a consequence of an instability of the power supply. Indeed, the current can be directly monitored by means of an optically coupled insulator in series with the current regulator [6], and the measured value of the current stability on a frequency range from DC to 2 MHz is better than 0.005 mA, that is one order of magnitude smaller than the range of settings explored in fig. 1.

We now show that two-peaked distributions depend on the statistical fluctuations of population inversion in the preparation process preceding the transient switch.

The class-B laser dynamics [12] can be described by two equations for the complex field amplitude $E = |E| \exp[i\phi]$ and population inversion Δ . We write the equations with the

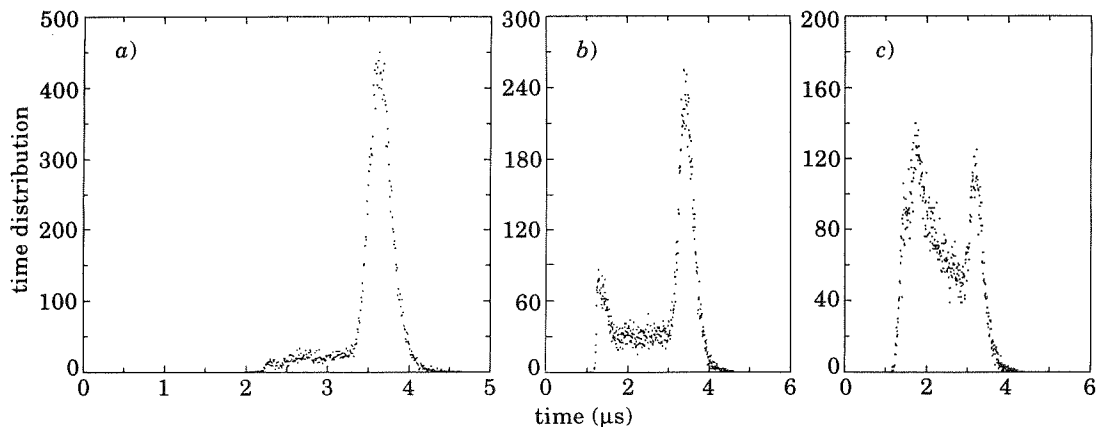


Fig. 1. – Experimental passage time distributions (10 000 trajectories) for the same final gain and for different initial settings close to threshold. The percentage current separations $\Delta i/i_{\text{th}}$ from the threshold value $i_{\text{th}} = 4.30 \text{ mA}$ are: -0.4% (a), -0.1% (b) and $+0.4\%$ (c), respectively. Notice that, for the sake of resolution, the horizontal scale in a) is different than in b), c).

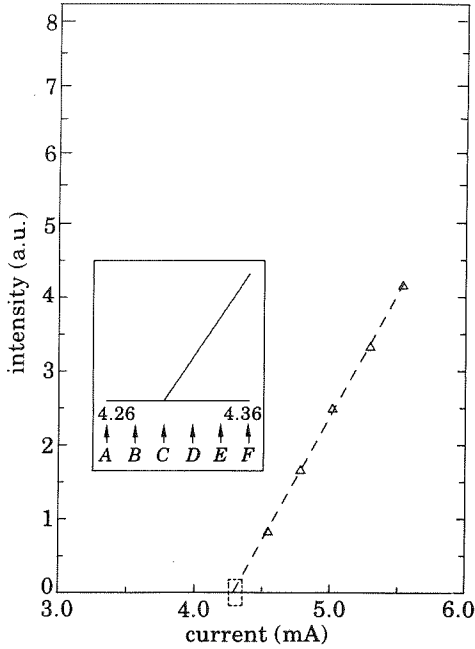


Fig. 2

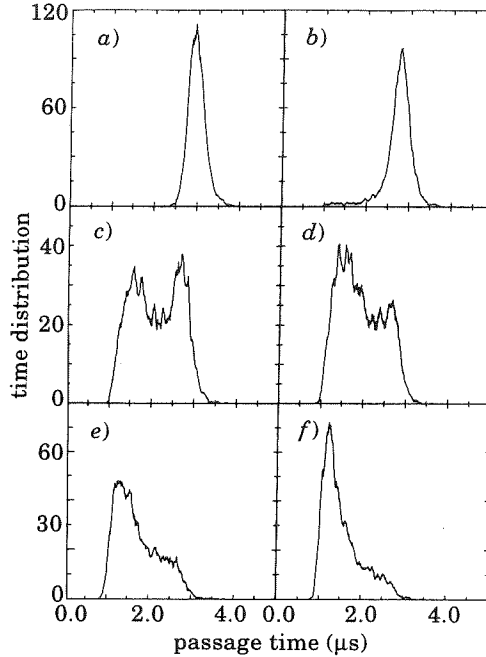


Fig. 3

Fig. 2. – Stationary laser output as a function of the discharge current at a fixed value $k = k_0$. Inset: expansion of the threshold region from 4.26 mA to 4.36 mA. The arrows indicate the discharge current values at which we have performed the numerical simulations reported in fig. 3.

Fig. 3. – Numerical results close to threshold. The percentage current separations $\Delta i/i_{th}$ from the threshold value $i_{th} = 4.30$ mA are: -0.93% (a)), -0.46% (b)), 0% (c)), 0.46% (d)), 0.93% (e)) and 1.4% (f)), respectively.

addition of two independent noise sources as follows:

$$\frac{dE}{dt} = -k(t)E + \frac{G\Delta E}{2} + (GN_2)^{1/2}\xi(t), \quad (1)$$

$$\frac{d\Delta}{dt} = -\gamma(\Delta - \Delta_0) - 2G\Delta|E|^2 + (R)^{1/2}\zeta(t), \quad (2)$$

where k is the decay rate of the field and $\gamma = 1.5 \cdot 10^4 \text{ s}^{-1}$ is the population decay rate. $\xi(t)$ and $\zeta(t)$ are two uncorrelated stochastic functions with zero mean value and δ -correlated in time. In the field equation the noise strength GN_2 is due to spontaneous emission, that is to radiative decay of the upper laser level population N_2 . In the population equation, the stochastic term of strength R accounts for several different sources such as gas composition, density and temperature fluctuations.

In order to compare the experimental results with the model, we have performed numerical simulations of the rate equations (1) and (2) with the stochastic Runge-Kutta method [13]. The following parameter values have been used: $k_0 = 1.977 \cdot 10^7 \text{ s}^{-1}$, $k_1 = 1.60 \cdot 10^7 \text{ s}^{-1}$, $GN_2 = 1.0 \cdot 10^9 \text{ s}^{-1}$, $R = 10^{29} \text{ s}^{-1}$. The first three are measured, R is chosen as follows. The «Brownian» part of eq. (2), that is $\dot{\Delta} = -\gamma\Delta + (R)^{1/2}\zeta(t)$, provides a r.m.s. fluctuation $\langle \Delta^2 \rangle^{1/2} = (R/\gamma)^{1/2} = 2 \cdot 10^{12}$ to be compared with $\Delta_0 \approx 9 \cdot 10^{14}$ (for $i = 4.30$ mA).

Hence the above R value corresponds to a relative population fluctuation $\langle \Delta^2 \rangle^{1/2} / \Delta_0 \approx 0.2\%$, sufficient to resolve the population steps reported in fig. 1. The spontaneous-emission contribution to the population noise, proportional to $-(2GN_2)^{1/2}$, is neglected with respect to the $R^{1/2}$ term, indeed $(2GN_2)^{1/2} / (R)^{1/2} \approx 10^{-10}$. The initial conditions for field and population are obtained after a thermalization time of $2.0 \cdot 10^{-4}$ s at $k(t) = k_0$. The integration step is 10^{-8} s.

Figure 3 shows simulated passage time distributions (5000 trajectories) around the threshold current in the presence of population inversion noise. Finally in fig. 4 we report the numerical results for $i = 4.30$ mA and $R = 0$ to confirm the essential role played by the population noise in determining two-peaked distributions. The narrow distribution of fig. 4 is a consequence of the fact that the initial laser state is always above threshold. Similar distributions have also been observed in the experiment [6] for $\Delta i / i_{th} > 2\%$, where the fluctuation μ is less relevant and cannot yield the initial state below threshold.

A theoretical explanation of the two-peak phenomenon was given in ref. [9] and is here summarized for the sake of completeness. In this stage of evolution, the field intensity $|E|^2$ is much smaller than the saturation intensity $n_s = \gamma / 2G$. The first approximation is then to consider $|E|^2$ as a constant in eq. (2). Therefore, we are able to solve the Fokker-Planck equation associated with eq. (2) in the steady state for $t < 0$ obtaining the probability density

$$P(\Delta) = c_1 \exp[-(\Delta - \bar{\Delta}_0)^2 / 2\sigma^2], \quad (3)$$

where c_1 is a normalization constant, and $\bar{\Delta}_0 = \Delta_0 / (1 + |E|^2 / I_s) \approx \Delta_0 (1 - |E|^2 / I_s)$, $\sigma^2 = (R/\gamma)(1 - |E|^2 / I_s)$. Equation (3) is a Gaussian distribution around the deterministic solution $\bar{\Delta}_0$ of eq. (2) and it implies that the value of population inversion for $t = 0$ can be written as

$$\Delta = \bar{\Delta}_0 + \eta, \quad (4)$$

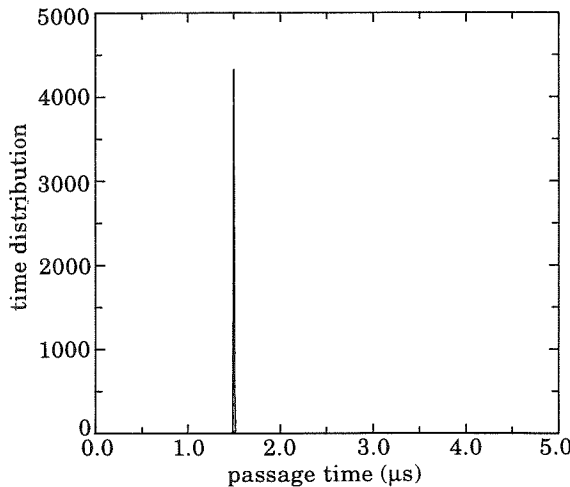


Fig. 4

Fig. 4. - Numerical results as in fig. 3c) with $R = 0$.

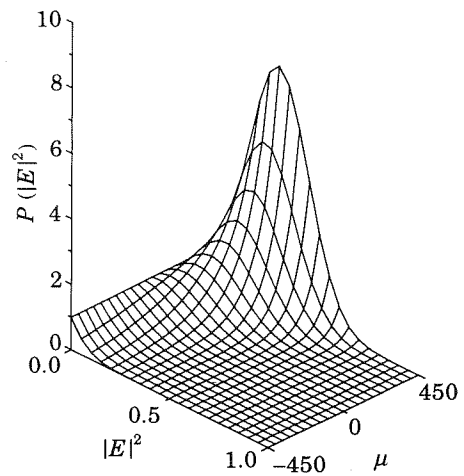


Fig. 5

Fig. 5. - Stationary distribution $P(|E|^2)$ vs. $|E|^2$ with $a_0 = 0$, $c_2 = 1$, $b = 1.21 \cdot 10^{-4}$ and $GN_2 = 1.0 \cdot 10^9$ for different realizations of the stochastic process μ . Horizontal scales: μ in s^{-1} , $|E|^2 = 1$ corresponds to $1.2 \cdot 10^8$ photons (notice that this photon number is still 10^{-3} times the saturation value).

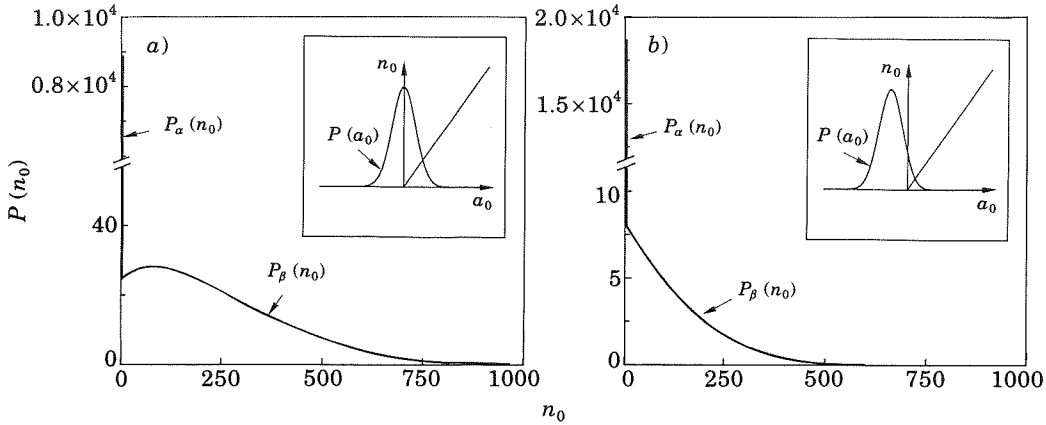


Fig. 6. – Initial distributions $P(n_0)$ for the photon number n_0 evaluated from the static curve n_0 vs. a_0 as given in fig. 2 (see insets, where we report also the spread $P(a_0)$ of the gain a_0 due to population fluctuations). Since the first packet $P_\alpha(n_0)$ is concentrated at $n_0 = 0$, the ratio of the two distributions α to β is here assigned in terms of the two integrated probability packets. Horizontal scales: $n_0 = 1000$ corresponds to $2.0 \cdot 10^9$. a) Two-peaked case, area ratio α to β : 0.8; b) single-peak case, area ratio α to β : 15.

where η is a Gaussian fluctuation with zero mean. Substituting eq. (4) into eq. (1) we obtain

$$\frac{dE}{dt} = (a_0 + \mu)E - b|E|^2E + (GN_2)^{1/2}\xi(t), \quad (5)$$

where $a_0 = G\Delta_0/2 - k_0$ is the laser net gain for $t < 0$ (that is, relative to the preparation process), $b = G^2\Delta_0/\gamma$ and $\mu = (G/2)\eta$. Equation (5) is a doubly stochastic equation because it has an additive noise source due to spontaneous emission and a multiplicative one due to population fluctuations. The stochastic term μ can be treated as a constant during each transient considering that the relaxation time $1/\gamma$ of the population is much longer than the duration of the transient itself. Thus, consideration of the preparation phase separately from the transient dynamics has led to eq. (5). A similar equation describes the role of coloured pump noise in a class-A laser [3]; in our case, however, it arises from an intrinsic population effect with no pump fluctuations.

For each realization of the process μ the steady-state solution of the Fokker-Planck equation associated with eq. (5) provides the initial field distribution from which the transient will start. This distribution, which results to be phase independent, is

$$(6) \quad P(|E|, \phi) = c_2 \exp \left[\left(\bar{a}_0 \frac{|E|^2}{2} - b \frac{|E|^4}{4} \right) / (GN_2) \right],$$

where $\bar{a}_0 = a_0 + \mu$ is the effective initial gain and takes different values for each of our experimental trajectories. c_2 is a normalizing factor. A plot of this distribution for different realizations of μ is given in fig. 5. Whenever $|a_0|$ is comparable with $\langle \mu^2 \rangle^{1/2}$ the initial-condition surface crosses the threshold $\bar{a}_0 = 0$, and the laser can start from below threshold (longer passage times) or above threshold (shorter passage times). Notice that

after the switch the fluctuations in μ evolve over a time scale fixed by the population decay rate γ , much longer than the transient.

Considering that $R = 4\gamma\langle\mu^2\rangle/G^2$, we obtain $\langle\mu^2\rangle^{1/2} = 6.00 \cdot 10^4 \text{ s}^{-1}$ which is comparable with the net gain a_0 of fig. 1 and 3b), c), d) ($|a_0| \leq 10^5 \text{ s}^{-1}$).

The above detailed explanation arising from eqs. (1) and (2) can be rephrased into a qualitative heuristic argument as follows. The preparation stage can be seen as the build-up of an initial photon population n_0 distributed according to the intensity *vs.* gain curve of fig. 2. Since the population fluctuations are equivalent to a spread $P(a_0)$ of the gain a_0 before the switch, placing $P(a_0)$ around the knee of the gain curve, we can roughly split this distribution into two packets, α and β , respectively, below and above the knee. This amounts to two classes of initial photon population, namely $P_\alpha(n_0)$ due to α and $P_\beta(n_0)$ due to β . Figure 6 shows two cases, one leading to a two-peak passage time distribution, because the combination of $P_\alpha(n_0)$ and $P_\beta(n_0)$ has two peaks, and one to a stretched distribution of passage times with only one peak. Thus, one can see the 1:1 correspondence between the behaviour of $P(n_0)$ and that of the passage time distribution.

* * *

We acknowledge relevant criticism from a referee which has led to substantial improvements. One of the authors (PYW) is the recipient of a fellowship from ICTP, Trieste (Italy). This work was partly supported by the E. C. Contract N° SC1*-CT91-0697 (TSTS).

REFERENCES

- [1] ARECCHI F. T., DEGIORGIO V. and QUERZOLA B., *Phys. Rev. Lett.*, **19** (1967) 1168; ARECCHI F. T. and DEGIORGIO V., *Phys. Rev. A*, **3** (1971) 1108.
- [2] ARECCHI F. T. and POLITI A., *Phys. Rev. Lett.*, **45** (1980) 1219.
- [3] ROY R., YU A. W. and ZHU S., *Phys. Rev. Lett.*, **55** (1985) 2794; DE PASQUALE F., SANCHO J. M., SAN MIGUEL M. and TARTAGLIA P., *Phys. Rev. Lett.*, **56** (1986) 2473.
- [4] MECOZZI A., PIAZZOLLA S., D'OTTAVI A. and SPANO P., *Phys. Rev. A*, **38** (1988) 3136; BALLE S., COLET P. and SAN MIGUEL M., *Phys. Rev. A*, **43** (1991) 498.
- [5] JAMES M., MOSS F., HÄNGGI P. and VAN DEN BROECK C., *Phys. Rev. A*, **38** (1988) 4690; TORRENT M. C. and SAN MIGUEL M., *Phys. Rev. A*, **38** (1988) 254.
- [6] ARECCHI F. T., MEUCCI R. and ROVERSI J. A., *Europhys. Lett.*, **8** (1989) 225; CIOFINI M., MEUCCI R. and ARECCHI F. T., *Phys. Rev. A*, **42** (1990) 482.
- [7] BROGGI G., COLOMBO A., LUGIATO L. and MANDEL P., *Phys. Rev. A*, **33** (1986) 3635; ZEGHLACHE H., MANDEL P. and VAN DEN BROECK C., *Phys. Rev. A*, **40** (1989) 286; TORRENT M. C., SANGUÈS F. and SAN MIGUEL M., *Phys. Rev. A*, **40** (1989) 6662; STOCKS N. G., MANNELLA R. and MCCLINTOCK P. V. E., *Phys. Rev. A*, **42** (1990) 3356.
- [8] SPANO P., MECOZZI A. and SAPIA A., *Phys. Rev. Lett.*, **64** (1990) 3003.
- [9] CIOFINI M., LAPUCCI A., MEUCCI R., PENG-YE WANG and ARECCHI F. T., *Phys. Rev. A*, **46** (1992) 5874.
- [10] YU A. W., AGRAWAL G. P. and ROY R., *J. Stat. Phys.*, **54** (1989) 1223.
- [11] SHEN T. M., *IEEE J. Lightwave Technology*, **7** (1989) 1394.
- [12] ARECCHI F. T., in *Instabilities and Chaos in Quantum Optics*, edited by F. T. ARECCHI and R. G. HARRISON (Springer-Verlag, Berlin, Heidelberg) 1987, p. 9.
- [13] HONEYCUTT R. L., *Phys. Rev. A*, **45** (1992) 600.